Available online at www.sciencedirect.com
ScienceDirect
Trans. Nonferrous Met. Soc. China 21(2011) 2705−2710
Transactions of Nonferrous Metals Society of China
www.tnmsc.cn

Theoretical analysis on springback of L-section extrusion in rotary stretch bending process

YU Cheng-long, LI Xiao-qiang

School of Mechanical Engineering and Automation, Beihang University, Beijing 100191, China

Received 19 November 2010; accepted 4 March 2011

Abstract: The theoretical analysis of springback in rotary stretch bending process of L-section extrusion was studied. The models for characterizing the springback angle after unloading were established based on the stress and strain distributions in the cross-section of the part. With the proposed model, analysis of the effect of pre-stretch force and post-stretch force on springback angle shows that springback decreases as the pre-stretch force or post-stretch force increases. Comparative study with experiments clearly demonstrates that the prediction of springback can resort to the current model without the loss of accuracy.
Key words: springback; rotary stretch bending; theoretical analysis

1 Introduction

Stretch bending is an important process for fabricating aircraft parts with large curvature in aerospace industry. In actual fabricating process, springback can lead to poor geometric accuracy and is often difficult to be controlled. It is thus of great importance to study the springback principle of stretch bending and the influence of process parameters on final shape of the part.

In recent decade, many research efforts have been focused on the issue. Experiment, theoretical analysis and finite element analysis are three main methods for predicting springback. MILLER et al [1−3] adopted the three means to investigate the effects of tension, internal pressure and friction on springback of rectangular aluminum tubes. Based on the experiment and finite element analysis, CLAUSEN et al [4−6] pointed out that the main factors that influence the springback include the yield criterion, material parameters (i.e., yield stress, strain hardening, plastic anisotropy), geometry parameters (i.e., die radius and wall thickness of section) and tensile sequence. PAULSEN and WELO [7] used commercial finite element software to study the effect of strain hardening and axial load on springback. Based on theoretical method, DU [8] analyzed bauschinger effect whereas ELSHARKAWY and EL-DOMIATY [9] explored the influence of the web thickness of T-section extrusions on springback. Furthermore, some researchers [10−12] used total strain theory to study the influence of external stretch force on springback. Besides, the software PS2F, which was specially developed on a perturbance analytical method for stretch bending, was also used in studying the springback [13, 14]. Recently, ZHU and STELSON [15] developed a simplified two-flange model for predicting the springback in stretch bending process. Verification showed that their model can lead to right variation tendency of the effect of pre-stretch force and post-stretch force on springback and indicated that the springback could be accurately controlled if control algorithm can be successfully applied to a stretch bending machine.

The present work is dedicated to a comprehensive study of the effects of pre-stretch force and post-stretch force on springback in rotary stretch bending (RSB) process of L-section extrusions. There are few works focused on modeling RSB. One available work is from YU and LIN [16], who analyzed the effect of pre-stretch force and side-pressure on springback in RSB using FEM. Although FEM is well known for its convenience of analyzing the sheet metal forming process, it behaves the feature of low efficiency with regard to real time control. To efficiently calculate the springback of RSB

Foundation item: Project (20090450276) supported by the China Postdoctoral Science Foundation; Project (50905008) supported by the National Natural Science Foundation of China
Corresponding author: YU Cheng-long; Tel: +86-15010285381, +86-10-82316584; E-mail: yuchengl@163.com
DOI: 10.1016/S1003-6326(11)61113-8

and further realize close-loop control of RSB, establishment of a simply computing model of springback is necessary.

The process of RSB is schematically illustrated in Fig. 1, from which it can be found that the two ends of the fabricated extrusion are gripped by the pre-stretch jaw and the post-stretch jaw, respectively. The working principle of RSB process is described as follows. Under a consecutive pre-stretch force loaded by pre-stretch jaw, the extrusion is continually bended as die and post-stretch jaw turn with rotary platform. Once the rotary platform turns to the designed position, an appropriate post-stretch force is applied to the extrusion through post-stretch jaw to accomplish the RSB process. This process consisted of pre-stretch process, bending process and post-stretch process. Springback will occur when the pre-stretch jaw and the post-stretch jaw are relaxed. The geometry of the L-section part is shown in Fig. 2.

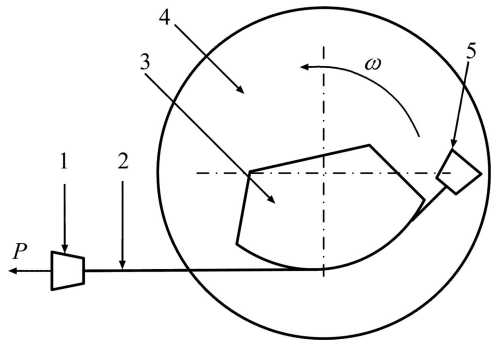

Fig. 1 Principle of RSB process: 1 — Pre-stretch jaw; 2 — Fabricated extrusion; 3 — Die; 4 — Rotary platform; 5—Post-stretch jaw (*P*: Pre-stretch force; *ω*: Angular velociety)

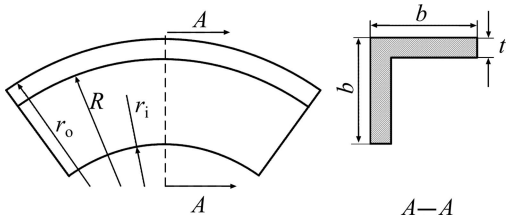

Fig. 2 Cross-section geometry (*b*: Width of extrusion section; *t*: Thickness of extrusion section)

2 Theoretical model

To develop the theoretical model of springback in the RSB process, the following assumptions are used.

1) The stress state is assumed to be uniaxial by ignoring the stress across the thickness of the section.

2) The cross-sectional shape does not change during the RSB process.

3) Bauschinger effect is neglected and the material property of the part is isotropic.

4) Friction effect between the part and the die is ignored.

5) The relationship between the stress σ and strain ε satisfies

$$\sigma=K\varepsilon^n \tag{1}$$

where K and n indicate the strength coefficient and the strain hardening exponent, respectively.

2.1 Analysis of pre-stretch process

The pre-stretch process is usually carried out by applying an axial tensional force T_y to the end of the part. Once this process is completed, the induced longitudinal stress σ_T and longitudinal strain ε_T meet the following relationship:

$$T_y = A\sigma_T \tag{2}$$

$$\sigma_T = K\varepsilon_T^n \tag{3}$$

where A is the area of the part cross-section.

2.2 Analysis of bending process

When the bending process is completed, the longitudinal stress in the cross-section will distribute like a piecewise function of the strain, as shown in Fig. 3. The symbols R, r_e, r_o, r_i and r_n in Fig. 3 mean the radius of curvature of die, lower limit of the elastic compression position, part outer surface, part inner surface and the position where the stress and strain are σ_T and ε_T after bending.

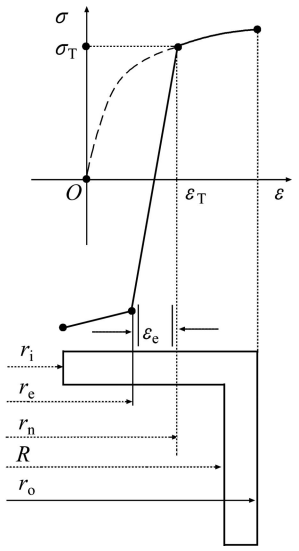

Fig. 3 Stress and strain distribution in cross-section after bending process

If $r_n \le r \le r_o$, σ_θ and ε_θ can be expressed as

$$\sigma_\theta = K(\varepsilon_T + \varepsilon_\theta)^n = \sigma_1 \tag{4}$$

where r means the radius of a certain position of the cross-section; ε_θ stands for the increment of longitudinal strain corresponding to r.

$$\varepsilon_\theta = (r - r_n)/r_n \tag{5}$$

If $r_e \le r \le r_n$, the part is in elastic compression state and σ_θ can be written as

$$\sigma_\theta = E\varepsilon_\theta + \sigma_T = \sigma_2 \tag{6}$$

Due to the fact that the Bauschinger effect is not considered, σ_2 equals $-\sigma_T$ when r achieves r_e. In this case, with the aid of Eq. (6), ε_θ can be calculated as

$$\varepsilon_\theta \triangleq \varepsilon_e = -2\sigma_T / E \tag{7}$$

where E is the elastic modulus of the part.

The substitution of $r=r_e$ and Eq. (7) into Eq. (5) will give

$$r_e = r_n(1+\varepsilon_e) \tag{8}$$

If $r_i \le r \le r_e$, the part is in yield of compression and σ_θ meets

$$\sigma_\theta = -K(\varepsilon_T + \varepsilon_e - \varepsilon_\theta)^n = \sigma_3 \tag{9}$$

According to the equilibrium of internal force and external force, one can have

$$T_y = b\int_R^{r_o} \sigma_1 \mathrm{d}r + t\int_{r_n}^{R} \sigma_1 \mathrm{d}r + t\int_{r_e}^{r_n} \sigma_2 \mathrm{d}r + t\int_{r_i}^{r_e} \sigma_3 \mathrm{d}r \tag{10}$$

where σ_1, σ_2 and σ_3 stand for the stress obtained from Eqs. (4), (6) and (9). r_o and r_i are calculated by

$$r_o = R + t \tag{11}$$

$$r_i = R - b + t \tag{12}$$

Now, by resorting to Eq. (10), the value of r_n can be solved. Subsequently, the longitudinal stress and strain distribution in a certain cross-section can be determined based on r_n.

2.3 Analysis of post-stretch process

At the initial stage of post-stretch process, the force on the post-stretch jaw has the same magnitude as the one on the pre-stretch jaw due to the fact that the friction is ignored. For the purpose of convenience, the post-stretch force T_p means the force increment applied to the post-stretch jaw. That is, the total force on the post-stretch jaw is the sum of the post-stretch force and the pre-stretch force. Under this definition, T_p will directly correspond to strain increment ε_p. According to Ref. [10], ε_p is assumed to be uniformly added to the part cross-section. One can have the following three stress-strain relationships based on the actual value of ε_p.

If $0 \le \varepsilon_p \le -\varepsilon_e$, $r_e \le r_{ep} \le r_n$, the stress—train relationship, as shown in Fig. 4 (a), can be mathematically written as

$$\sigma_\theta = \begin{cases} K(\varepsilon_T + \varepsilon_\theta + \varepsilon_p)^n \triangleq \sigma_a, & \text{if } r_{ep} \le r \le r_o \\ E\varepsilon_p + \sigma_2 \triangleq \sigma_b, & \text{if } r_e \le r \le r_{ep} \\ E\varepsilon_p + \sigma_3 \triangleq \sigma_c, & \text{if } r_i \le r \le r_e \end{cases} \tag{13}$$

$$\text{with} \quad r_{ep} = r_n(1-\varepsilon_p) \tag{14}$$

where r_{ep} represents the radius of the elastic-plastic interface after post-stretch process.

The equilibrium of internal force and external force gives rise to

$$T_y + T_p = b\int_R^{r_o} \sigma_a \mathrm{d}r + t\int_{r_{ep}}^{R} \sigma_a \mathrm{d}r + t\int_{r_e}^{r_{ep}} \sigma_b + t\int_{r_i}^{r_e} \sigma_c \mathrm{d}r \tag{15}$$

If $-\varepsilon_e \le \varepsilon_p$, $r_i \le r_{ep} \le r_e$, the stress—train will have the distribution form as shown in Fig. 4 (b) and can be

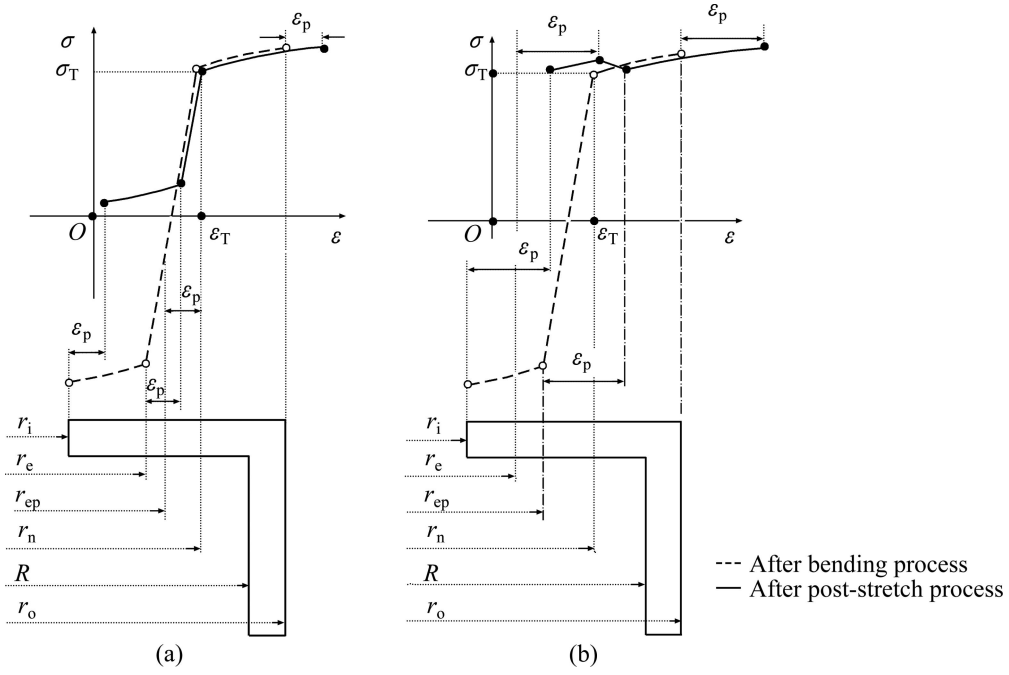

Fig. 4 Stress and strain distributions in cross-section after post-stretch process: (a) $0 \le \varepsilon_p \le -\varepsilon_e$, $r_e \le r_{ep} < r_n$; (b) $-\varepsilon_e \le \varepsilon_p$, $r_i \le r_{ep} < r_e$

expressed as

$$\sigma_\theta=\begin{cases}K(\varepsilon_T+\varepsilon_\theta+\varepsilon_p)^n \triangleq \sigma_a, \text{if } r_e\le r\le r_o\\ K[\varepsilon_T+\varepsilon_e-\varepsilon_\theta+(\varepsilon_p-\varepsilon_{ep})]^n \triangleq \sigma_b, \text{if } r_{ep}\le r\le r_e\\ E\varepsilon_p+\sigma_3 \triangleq \sigma_c, \text{if } r_i\le r\le r_{ep}\end{cases} \tag{16}$$

where ε_{ep} is the strain increment of the section loaded from the yield of compression to the yield of tension. It can be written as

$$\varepsilon_{ep}=2K\left(\varepsilon_T+\varepsilon_e-\varepsilon_\theta\right)^n/E \tag{17}$$

The relationship between ε_p and r_{ep} is

$$\varepsilon_p=2K[\varepsilon_T+\varepsilon_e-\left(r_{ep}-r_n\right)/r_n]^n/E \tag{18}$$

Similarly, according to equilibrium principle, the internal force and external force will follow

$$T_y+T_p=b\int_R^{r_o}\sigma_a\mathrm{d}r+t\int_{r_e}^{R}\sigma_a\mathrm{d}r+t\int_{r_{ep}}^{r_e}\sigma_b+t\int_{r_i}^{r_{ep}}\sigma_c\mathrm{d}r \tag{19}$$

Once the post-stretch force is large enough, r_{ep} will be less than r_i. In this case, one can have

$$\sigma_\theta=\begin{cases}K(\varepsilon_T+\varepsilon_\theta+\varepsilon_p)^n \triangleq \sigma_a, \text{if } r_e\le r\le r_o\\ K[\varepsilon_T+\varepsilon_e-\varepsilon_\theta+(\varepsilon_p-\varepsilon_{ep})]^n \triangleq \sigma_b, \text{if } r_i\le r\le r_e\end{cases} \tag{20}$$

The equilibrium equation of internal force and external force is

$$T_y+T_p=b\int_R^{r_o}\sigma_a\mathrm{d}r+t\int_{r_e}^{R}\sigma_a\mathrm{d}r+t\int_{r_i}^{r_e}\sigma_b \tag{21}$$

Now, as long as post-stretch force T_p, the geometry parameters of the part and the radius of die are given, ε_p can be easily solved from Eqs. (15), (19) or (21). Subsequently, the longitudinal stress—strain distribution in the cross-section after post-stretch force can be determined based on ε_p.

2.4 Analysis of springback process

Springback phenomenon will occur once the pre-stretch jaw and post-stretch jaw are relaxed.

1) If no post-stretch force is loaded, the bending moment M can be written as

$$M=b\int_R^{r_o}\sigma_1\left(r-r_z\right)\mathrm{d}r+t\int_{r_n}^{R}\sigma_1(r-r_z)\mathrm{d}r+t\int_{r_e}^{r_n}\sigma_2(r-r_z)\mathrm{d}r+t\int_{r_i}^{r_e}\sigma_3(r-r_z)\mathrm{d}r \tag{22}$$

where r_z is the curvature radius of the centroid of the L-section extrusion before the force is unloaded.

2) If post-stretch force is loaded, M can be expressed as

$$M=\begin{cases}b\int_R^{r_o}\sigma_a\left(r-r_z\right)\mathrm{d}r+t\int_{r_{ep}}^{R}\sigma_a\left(r-r_z\right)\mathrm{d}r+\\ \quad t\int_{r_e}^{r_{ep}}\sigma_b\left(r-r_z\right)\mathrm{d}r+t\int_{r_i}^{r_e}\sigma_c\left(r-r_z\right)\mathrm{d}r,\\ \quad r_e\le r_{ep}\le r_n\\ b\int_R^{r_o}\sigma_a\left(r-r_z\right)\mathrm{d}r+t\int_{r_e}^{R}\sigma_a\left(r-r_z\right)\mathrm{d}r+\\ \quad t\int_{r_{ep}}^{r_e}\sigma_b\left(r-r_z\right)\mathrm{d}r+t\int_{r_i}^{r_{ep}}\sigma_c\left(r-r_z\right)\mathrm{d}r,\\ \quad r_i\le r_{ep}\le r_e\\ b\int_R^{r_o}\sigma_a\left(r-r_z\right)\mathrm{d}r+t\int_{r_e}^{R}\sigma_a\left(r-r_z\right)\mathrm{d}r+\\ \quad t\int_{r_i}^{r_e}\sigma_c\left(r-r_z\right)\mathrm{d}r, r_{ep}\le r_i\end{cases} \tag{23}$$

3) Calculation of springback angle. Assume that axial strains are negligible during unloading according to Ref. [6]. Thus, the following equation can be obtained:

$$\alpha_z r_z=\alpha_h r_h \tag{24}$$

where α_z and α_h are the bending angles before and after the force is unloaded, as shown in Fig. 5; r_h is the curvature radius of the centroid of the L-section extrusion after the force is unloaded. The springback angle $\Delta\alpha$ can be written as

$$\Delta\alpha=\alpha_z-\alpha_h=(1-r_z/r_h)\alpha_z \tag{25}$$

The relationship between r_z and r_h can be expressed as

$$1/r_z-1/r_h=M/(EI) \tag{26}$$

By reviewing Eq. (25) and Eq. (26), the relationship between $\Delta\alpha$ and M can be derived as

$$\Delta\alpha=r_z\alpha_z M/(EI) \tag{27}$$

where I is the inertia moment of the L-section.

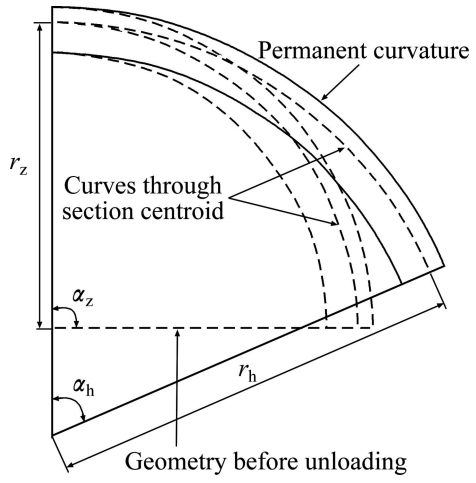

Fig. 5 Definition of springback angle

3 Experiment of RSB process

Experiments are performed on the RSB machine with the curvature radius of the die of 200 mm, as shown in Fig. 6. The part material is aluminum alloy LY12M-XC111-37 with strength coefficient K=276.21 MPa, strain hardening exponent n=0.123, and elastic modulus E=72986.01 MPa. The parameters related to the L-section of the part are: b=30 mm, t=2 mm, r_z=193.76 mm, I=10195.91 mm^4. The length of the profile is 1 500 mm. The angle of the rotary platform turning (α_z) is 90°. α_h is measured on the outer surface of the flange. Then, the springback angle $\Delta\alpha$ can be calculated by Eq. (25). The experiment results and the parameters of pre-stretch force and post-stretch force are listed in Table 1.

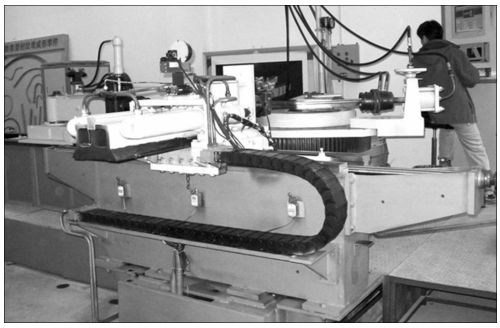

Fig. 6 RSB machine

Table 1 Experiment results

T_p=0 N		T_y =16 kN		T_y =13 kN	
T_y/kN	$\Delta\alpha$/(°)	T_p/kN	$\Delta\alpha$/(°)	T_p/kN	$\Delta\alpha$/(°)
16	4.36	1	3.40	5	3.71
17	3.50	2	3.99	6	3.11
18	3.10	3	3.37	7	2.54
19	2.50	4	2.51	8	2.13
20	2.10	5	2.26	9	1.75

4 Results and discussion

4.1 Comparison between experimental and theoretical results without post-stretch force

Before the post-stretch force is applied, the relationship between springback angle and pre-stretch force shows that there is a relatively good agreement between the experiment results and the theoretical ones, as shown in Fig. 7. As the pre-stretch force increases, both the measured and predicted springback angles show decrease tendency whereas the deviation between both results will increase. The reason can be attributed to the following fact. In the theoretical analysis procedure, the cross-sectional shape is assumed to be not changed during the RSB process, whereas in the actual process, the area of the cross-section decreases as the pre-stretch force increases. As a result, the actual stress of the cross-section will be larger than the theoretical one, and the deviation between the experiment stress and theoretical one will increase as the pre-stretch force increases.

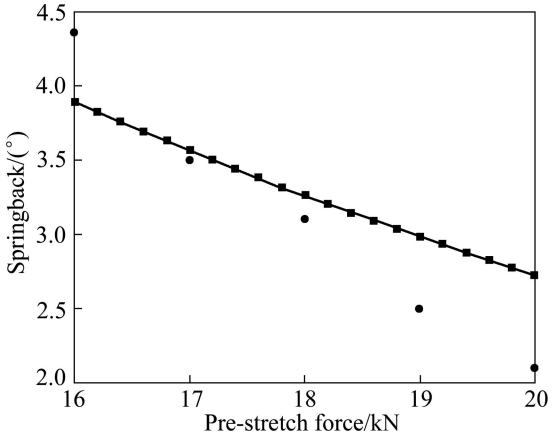

Fig. 7 Springback varying with pre-stretch force

4.2 Comparison between experimental and theoretical results with post-stretch force

Figure 8 shows that the post-stretch force can also

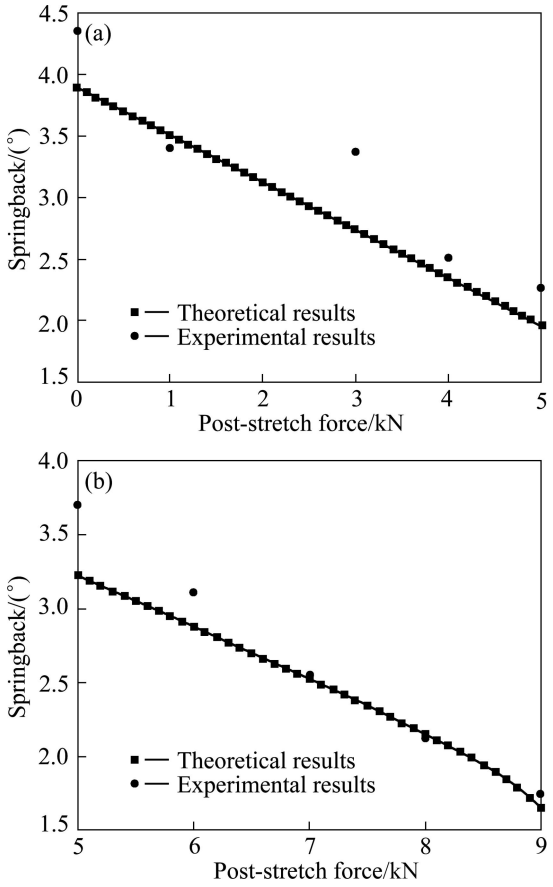

Fig. 8 Springback varying with post-stretch force at different pre-stretch forces: (a) 16 kN; (b) 13 kN

lead to the reduction of springback. If the post-stretch force is small, the experiment results are larger than the theoretical ones, as shown in Fig. 8(a). The cause of this may be due to the following point. On the one hand, when the post-stretch force is applied to the extrusion after bending, the friction will weaken the transmission of the post-stretch force from the post-stretch jaw to the extrusion. As a result, the actual value of stretch is less than the theoretical one. On the other hand, the effect of friction on the actual stress is greater than the effect induced by the reduction of the cross-sectional area, as discussed in Section 4.1. As the post-stretch force increases, the calculated results are in a very good agreement with the experiment ones, as shown in Fig. 8(b). This may be due to the fact that the positive effect of cross-section area reduction and the negative effect of friction are in an equilibrium state. Besides, the springback angle at 1 kN, as shown in Fig. 8(a), is less than the predicted one due to the drift of the setup in the process.

5 Conclusions

1) The calculated results of springback angle are in a relatively good agreement with experimental one based on the proposed method. The springback shows decrease tendency as the pre-stretch force or post-stretch force increases.

2) Stress and strain distributions in cross-section are presented based on the theoretical model. This can be helpful to understand the forming theory of RSB. The theoretical model of L-section extrusion could be extended to other sectional extrusions such as U-section and T-section.

3) The model might be suitable for closed loop control in the future.

References

[1] MILLER J E, KYRIAKIDES S, BASTARD A H. On bend-stretch forming of aluminum extruded tubes-I: Experiments [J]. International Journal of Mechanical Sciences, 2001, 43: 1283−1317.

[2] MILLER J E, KYRIAKIDES S, CORONA E. On bend-stretch forming of aluminum extruded tubes-II: Analysis [J]. International Journal of Mechanical Sciences, 2001, 43: 1319−1338.

[3] MILLER J E, KYRIAKIDES S. Three-dimensional effects of the bend-stretch forming of aluminum tubes [J]. International Journal of Mechanical Sciences, 2003, 45: 115−140.

[4] CLAUSEN A H, HOPPERSTAD O S, LANGSETH M. Stretch bending of aluminum extrusions: Effect of geometry and alloy [J]. ASCE Journal of Engineering Mechanics, 1999, 125: 392−400.

[5] CLAUSEN A H, HOPPERSTAD O S, LANGSETH M. Stretch bending of aluminum extrusions: Effect of tensile sequence [J]. ASCE Journal of Engineering Mechanics, 1999, 125: 521−529.

[6] CLAUSEN A H, HOPPERSTAD O S, LANGSETH M. Sensitivity of model parameters in stretch bending of aluminium extrusions [J]. International Journal of Mechanical Sciences, 2001, 43: 427−453.

[7] PAULSEN F, WELO T. Application of numerical simulation in the bending of aluminum-alloy profiles [J]. Journal of Materials Processing Technology, 1996, 58: 274−285.

[8] DU Song. Influence of bauschinger effect on springback in sheet metal stretch bending [J]. Journal of Beijing University of Aeronautics and Astronautics, 2007, 33(2): 206−209. (in Chinese)

[9] ELSHARKAWY A A, EL-DOMIATY A A. Determination of stretch-bendability limits and springback for T-section beams [J]. Journal of Materials Processing Technology, 2001, 110: 265−276.

[10] KUWABARA T, TAKAHASHI S, AKIYAM K, MIYASHITA Y. 2-D springback analysis for stretch-bending processes based on total strain theory [J]. SAE Transactions Section 5, 1995, 950691: 504−513.

[11] ZHANG Dong-juan, CUI Zhen-shan, LI Yu-qiang, RUAN Xue-yu. Springback of sheet metal after plane strain stretch-bending [J]. Engineering Mechanics, 2007, 24(7): 66−71. (in Chinese)

[12] QIAN Zhi-ping, ZHOU Chao, ZHAO Jun, GAO Cai-liang, LÜ Mei. Springback research for stretch bending of aluminum profile cover with plastics [J]. Journal of Plasticity Engineering, 2008, 15(3): 77−80. (in Chinese)

[13] JIN Chao-hai, ZHOU Xian-bin. PS2F-based study on springback in stretch-wrap bending of aluminum profiles [J]. Journal of Plasticity Engineering, 2007, 14(3): 1−4. (in Chinese)

[14] GU Zheng-wei, CAI Zhong-yi, XU Hong. Numerical analysis and optimization of stretch-bending process [J]. Journal of Jilin University: Engineering and Technology Edition, 2009, 39(5): 1167−1171. (in Chinese)

[15] ZHU H, STELSON K A. Modeling and closed-loop control of stretch bending of aluminum rectangular tubes [J]. Journal of Manufacturing Science and Engineering, 2003, 125: 113−119.

[16] YU Zhong-qi, LIN Zhang-qin. Numerical analysis of dimension precision of U-shaped aluminium profile rotary stretch bending [J]. Transactions of Nonferrous Metals Society of China, 2007, 17(3): 581−585.

角型材转台式拉弯回弹的解析分析

于成龙，李小强

北京航空航天大学 机械工程及自动化学院，北京 100191

摘 要：从理论上对角型材的拉弯回弹进行研究，基于角型材截面应力、应变分布算法建立拉弯解析模型，推导零件卸载后回弹角的计算公式，分析讨论预拉力和补拉力对回弹的影响规律。结果表明：拉弯零件的回弹随着预拉力或补拉力的增大而减小。与试验结果的对比表明，建立的解析模型能够较好地预测角型材拉弯零件的回弹。

关键词：回弹；转台式拉弯；解析分析

(Edited by LI Xiang-qun)